JAIST Repository
https://dspace.jaist.ac.jp/

Title	Attribution of H+ Transportation of Nafion-Film on Different Substrates Using Planar Inter-Digitated Electrodes
Author(s)	Bhardwaj, Rahul; Karan, Kunal; Nagao, Yuki
Citation	ECS Transactions, 109(9): 303
Issue Date	2022-10
Type	Journal Article
Text version	author
URL	http://hdl.handle.net/10119/18790
Rights	Copyright (C)2022 ECS. Rahul Bhardwaja, Kunal Karanb, and Yuki Nagao, ECS Transactions, 109 (9), 2022, pp.303. This work is available under the Creative Commons Attribution-NonCommercial-NoDerivatives 4.0 International license (CC BY-NC-ND 4.0) [http://creativecommons.org/licenses/by-nc-nd/4.0/]. This is the Accepted Manuscript version of an article accepted for publication in ECS.
Description	

JAIST
JAPAN
ADVANCED INSTITUTE OF
SCIENCE AND TECHNOLOGY

Japan Advanced Institute of Science and Technology

Attribution of H^+ Transportation of Nafion-Film on Different Substrates Using Planar Inter-Digitated Electrodes

Rahul Bhardwaj[a], Kunal Karan[b], and Yuki Nagao[a*]

[a]School of Materials Science, Japan Advanced Institute of Science and Technology, 1-1 Asahidai, Nomi city, Ishikawa, 923-1292, Japan

[b]Calgary Advanced Energy Storage and Conversion Research–Technologies (CAESR-Tech) Group, The University of Calgary, 2500 University Dr. NW, Calgary, T2N 1N4, Canada

In-plane proton transport property of Nafion thin-film on carbon and quartz was investigated in N_2 environment by electrochemical impedance spectroscopy (EIS) using interdigitated electrodes (IDEs) of platinum on quartz substrate. The Pt IDEs with and without carbon pad were fabricated with precise geometry and excellent current-voltage (I-V) response in few hundreds femtoampere (fA). The morphology of spin-coated Nafion thin-film over IDEs was confirmed to adapt the geometry of IDE structure. The EIS impedance response of Nafion thin-film consists of single semi- circular component in either IDEs. Since Pt-C IDE has both ionomer/quartz and ionomer/carbon interface therefore H^+ conductivity at quartz and carbon was estimated from the quantitative attribution of H^+ transport resistance. The estimated H^+ conductivity at quartz from Pt-C IDE and Pt-Q IDE shows comparable conductivity values except the high relative humidity (RH) and indicates that H^+ transport resistance at carbon substrate in Pt-C IDE is absent in N_2 environment.

Introduction

Proton transport is a key functional property of the ionomer used in energy device (1–3). Nafion is the most extensively employed ionomer which serves as free standing membrane and as thin film coating the electrocatalyst in polymer electrolyte membrane-

based fuel cell (PEMFC) (4–6). In the cathode catalyst layer of PEMFC, thin film of ionomer plays crucial role and determines the performance of fuel cell. In a fuel cell catalyst layer, ionomer thin films coating the carbon-supported Pt-based catalysts (Pt/C) is distributed in 3D spatially heterogeneous manner with variation in thickness and connectivity (7). Recently, Nafion thin-film has attracted attention and have been extensively investigated because of different phase segregated structure and proton transport property compared to thick Nafion membrane (8–18). It is now well established that hydration and proton conduction properties of Nafion films are thickness- and substrate-dependent. Because of their non-uniform distribution (varying thickness and connectivity) as well as interfacing with different substrates (carbon and Pt), it is difficult to clarify the quantitative attribution of the true source of effective proton resistance. Despite the tremendous significance of ionomer thin film in fuel cell and other energy devices, the efforts to explore the quantitative attribution of substrate-dependance on H^+ conductivity has not sufficiently advanced. Only a handful of studies had been reported about the influence of substrate and confinement effect on the structure and property of Nafion's thin films specifically wherein conductivity of ionomer film of uniform and controlled thickness on well-defined planar substrate has been reported. These studies have focused on understanding the morphology or proton conductivity of the Nafion thin films, the quantitative relationship between morphology and proton conductivity of the Nafion thin films on Pt and/or carbon substrates has not been clarified (16,19–23). Yamamoto's group has investigated the substrate dependent H^+ conductivity of uniform and controlled Nafion thin film using Au-IDE with Pt and C pad in N_2 environment and shows that Pt-supported Nafion thin-film exhibited higher H^+ conductivity than carbon supported Nafion films (22). Our group, Ono et. al., has also investigated the H^+ conductivity at Pt and SiO_2 substrate using parallel Au electrodes and concluded that H^+ conductivity on Pt deposited surface was one order of magnitude higher than that on SiO_2 (23). Karan's group has extended the investigation with more details using planar Pt-IDEs in N_2 and H_2 environment and concluded that the protonic resistance of the ionomer thin-film on top of conductive substrate is not accessible unless measurement was performed under H_2 environment using Pt electrodes (21,24). However, despite the larger area between IDE was covered with substrate material (ionomer/substrate interface), the attribution of H^+ transport at ionomer/quartz part was absent in their work.

In this work, we are using planar interdigitated electrodes of Pt with fixed thickness

of Nafion. Electrochemical Impedance Spectroscopy (EIS) was employed for impedance measurement of the Nafion thin film on inter-digitated array (IDA) of Pt electrode with and without carbon pad between the electrodes. Film resistance as a function of relative humidity was determined. The proton transport resistance from EIS was quantitatively attributed based on the ionomer/substrate interfacial area to estimate the Nafion thin-film proton conductivity over quartz and carbon substrate. A comparison of the conductivity of the Nafion thin film on carbon and quartz in N_2 environment is reported and discussed.

Experimental Section

IDE Fabrication

A schematic fabrication process of the Pt IDEs with carbon pad (step 1-8) and without carbon pad (step 1, 6-8) is illustrated in Fig. 1, and referred to as Pt-C IDE and Pt-Q IDE respectively (Q stands for quartz). The IDE has 108 substrate carbon pads of 100-µm width with 120 µm-pitch. Firstly, the quartz substrates (20 × 20 × 0.5 mm) were cleaned by sonication in acetone (EL grade) and isopropyl alcohol (EL grade) for 5 and 10 min each. The quartz substrates were cleaned with piranha solution followed by running mili-Q (Ultrapure) water to remove deposited organic impurities only if the substrates were used for high temperature pyrolysis process. The 1,1,1,3,3,3-hexamethyldisilazane (HMDS) solution was spin coated to improve the adhesion before photoresist coating. The 30% v/v AZP 4210 photoresist (diluted with AZ EBR7030 solvent) was spun coated at 3000 rpm for 150 s and pre-annealed at 110℃ for 90 s. To prepare the carbon pad pattern out of photoresist film, a maskless aligner system (MLA150 HEIDELBERG-instruments) was used for photolithography and then developed in NMD-3 reagent for 55 s. The quartz with photoresist pattern was plasma exposed in O_2 for 20 s at 15 W to remove residual resist nanofilm between patterns. The patterned photoresist was carbonized at 1000 ℃ in 2% H_2/N_2 environment. The quartz substrate with carbonized patterns was again exposed to plasma for 20 s at 15 W. After that, the electrodes were prepared by the lift-off process. The LOL-2000 and TSMR-8900 (20cp) photoresist was spin coated at 3000 rpm for 30 s and dried at 110℃ for 90 s before lithography. The Pt was physically deposited by sputtering at 100 ℃ for 12 min with Ti (~2-5 nm) as adhesion layer.

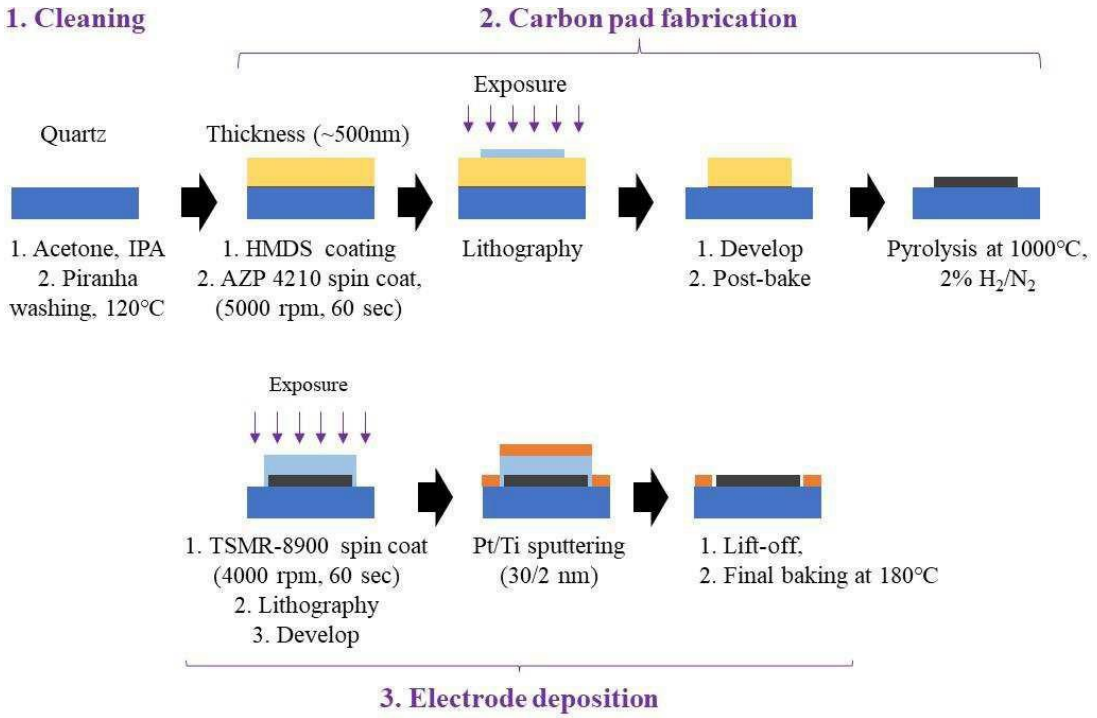

Figure 1. A schematic step by step illustration of IDEs fabrication process.

Thin-Film Preparation

The 5wt% Nafion dispersion stock solution (DE521 CS type; Wako Pure Chemical Industries Ltd.) was diluted to 1.2wt% in isopropyl alcohol and sonicated for 30 min. The dispersion was equilibrated for 24 h. Before ionomer coating, IDEs were again washed with acetone and IPA by sonication followed by plasma treatment (Cute-MP; Femto Science, Korea), and ionomer dispersion was ultrasonicated for 15 min. The Nafion's thin film was prepared from diluted dispersion concentration by spin-coating method (ACT-200; Active) at room temperature. After coating, Nafion's film outside the IDE structure was removed manually with a swab using Mili-Q water and film was dried at 40℃ under vacuum overnight.

IDE Characterizations and Thin-Film Thickness Measurement

After fabrication, IDE alignment precision was confirmed using an optical microscope (Company name). The I-V response in the range of 0-1 V using semiconductor parameter analyzer (E5250A Agilent) and a measurement probe (TN-1910 Vector Semiconductor) was recorded to check the resistance of interdigitated electrodes

with and without carbon pad. The thickness of carbon pad, Pt electrode and ionomer thin film coated on IDEs was measured using white light interferometric microscope (BW-S506; Nikon Corp.) and AlphaStep D-100 surface profiler (KLA Tencor).

Nafion Thin Film Conductivity Measurement

A small humidity box was newly constructed for thin-film H^+ conductivity measurement in a humidified N_2 environment. All measurements were conducted at temperature 25 ℃ (controlled using a computer-controlled chamber SH-221; Espec Corp.) under various RH generated by separate humidity generator (me-40DP-2PW; Micro Equipment Inc.). For thin-film impedance measurement, a two-probe method was applied to obtain in-plane proton conductivity parallel to the thin-film. Thin gold wires (dia 0.5μm, Y-soft Tanaka Denshi Kogyo K. K. Japan) were used to connect probes with Pt electrodes contact pad using porous gold paste (SILBEST No. 8560; Tokuriki Chemical Research Co. Ltd.). Impedance data were collected at alternating amplitude frequency of 50 mV and frequency range from 10 MHz and 0.1 Hz. The Nafion thin-film resistance was obtained from collected impedance data using the semi-circle fitting method and line fitting method in ZView software (version 3.3f). The H^+ conductivity of thin film (σ) was calculated from the resistance (R) measured on IDEs using the following equation [1].

$$\sigma = \frac{d}{R*L*(N-1)*w} \quad [1]$$

In the above equation [1] denotes the gap between Pt electrodes (110 μm), L is dry thickness of Nafion thin film (~55 nm), N is the number of electrodes (109), and w is width of Pt electrode (8 mm).

Before the measurement was initiated, the film was dried completely at 40 ℃ overnight under vacuum to remove moisture from the film. During the vacuum drying, the relative humidity inside the vacuum chamber was approximately 3%. The in-plane proton transport impedance of Nafion film was measured at various relative humidity starting from 20% up to 95% using humidity generator in N_2 atmosphere. Before EIS measurement, IDEs with Nafion thin film was kept in dry N_2 environment for 1h to remove any remaining moisture from the film. During dry N_2 flow, humidity reaches to 5% and expected to remove moisture from chamber and film. The humidity was increased sequentially starting from 20% and impedance was recorded at each RH until stabilized.

Results and Discussions

IDE Fabrication

The optical microscope images of fabricated IDE with their specification are presented in Figure 2. Neither apparent micro-defect nor cracks were observed on carbon pad and Pt confirming that the device structure was successfully fabricated. Moreover, precise alignment of the device was achieved. The carbon pads have length (L) and width (w) of 8 mm and 100 µm respectively and precisely aligned between Pt IDE at 5 µm distance from each Pt electrode of 10 µm width. This clean and precise fabrication of IDEs is an important feature to achieve the reproducibility of Nafion thin film H^+ conductivity. The current-voltage response of IDEs (with and without carbon pad) in range of 0-1 V was recorded ~100 fA (Data is not shown here). It shows high resistance of fabricated IDEs with Pt electrodes distanced at 110 µm, and the introduction of conductive carbon pad distanced at 5 µm from Pt electrodes at both sides doesn't influence the I-V response. The I-V response of IDEs also supports the high resistance of quartz substrate between electrodes. The thickness of the carbon pad and sputtered Pt electrode was measured using a surface profiler and showed 30 nm and 35 nm respectively. Top photograph of the Pt-C and Pt-Q IDE is also shown in Fig. 2.

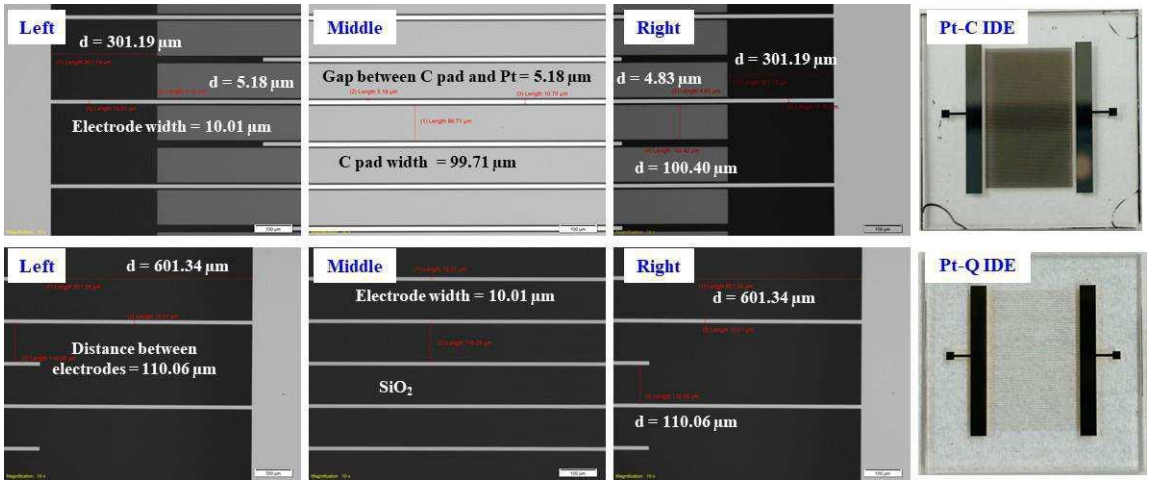

Figure 2. Optical microscope images of different parts from fabricated IDEs with geometry measurement and photograph of Pt-C IDE and Pt-Q IDE.

Nafion Thin-Film Characterization

The Nafion thin film of ~55 nm thickness was optimized from various concentration dispersions and film thickness was confirmed by white light microscope and surface profiler (data not shown here). After spin coating over IDE, film thickness and morphology of thin film were analyzed using surface profiler (applied stylus force of 0.3 mg). Figure 3 (a & b) shows the illustration of expected and measured Nafion film morphology over the Pt-C IDE. In the illustrations (Fig. 3), Nafion film is shown over IDE structure only because Nafion film other than IDE structure was manually removed using swab and mil-Q. The Nafion thin film was expected to have flat morphology over IDE however the measured film morphology was surprisingly seeming to adapt the exact morphology of IDEs. It is the first time to report the morphology of Nafion film over an IDE for H^+ conductivity measurement. In surface profiler data (Fig. 3c), the thickness of Nafion film at the edge is slightly thicker resulting from film accumulating during swab removal. The sharp peaks shown in Nafion film surface profile is the result of system measurement error. Film thickness over IDE was determined to be around 60 nm from profiler data (confirmed by white light microscope, data not shown here).

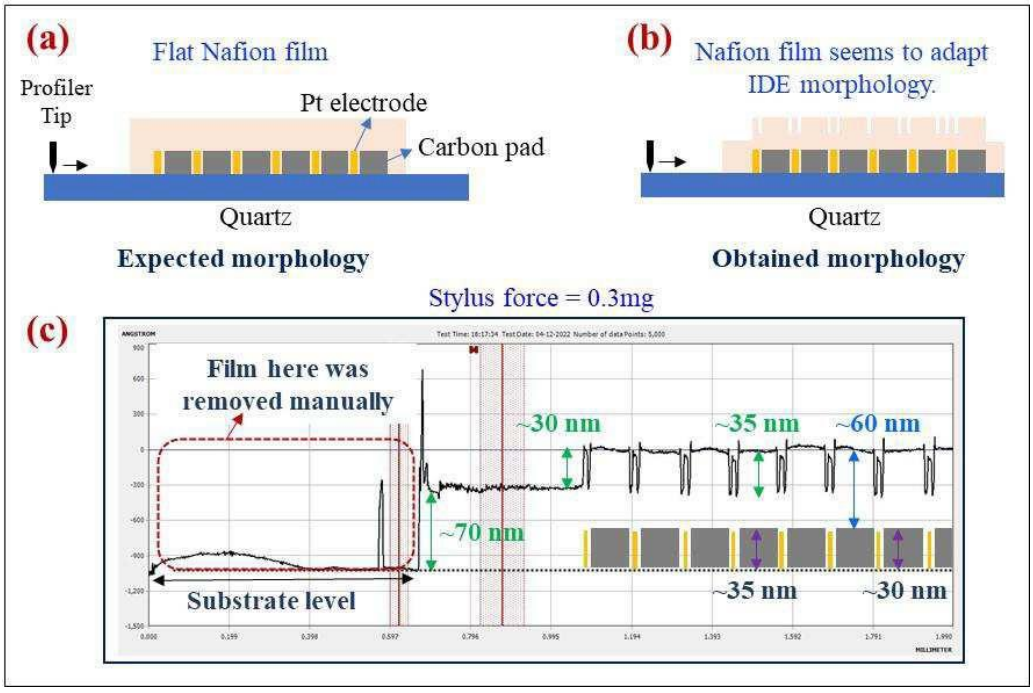

Figure 3. (a & b) Illustrations of Nafion's thin film expected morphology and obtained film morphology on IDEs. (C) Nafion thin film's thickness and morphology over IDE measured by surface profiler with stylus force of 0.03 mg with 0.1 mm/sec speed rate.

Impedance Measurement of Nafion Film using IDEs

The impedance response of Nafion's thin film consists of an inductive part, a semicircle at the high-frequency region (corresponds to H^+ resistance at substrate) and a vertical-line like response in the low frequency region (corresponds to infinite diffusion) (Fig. 4).

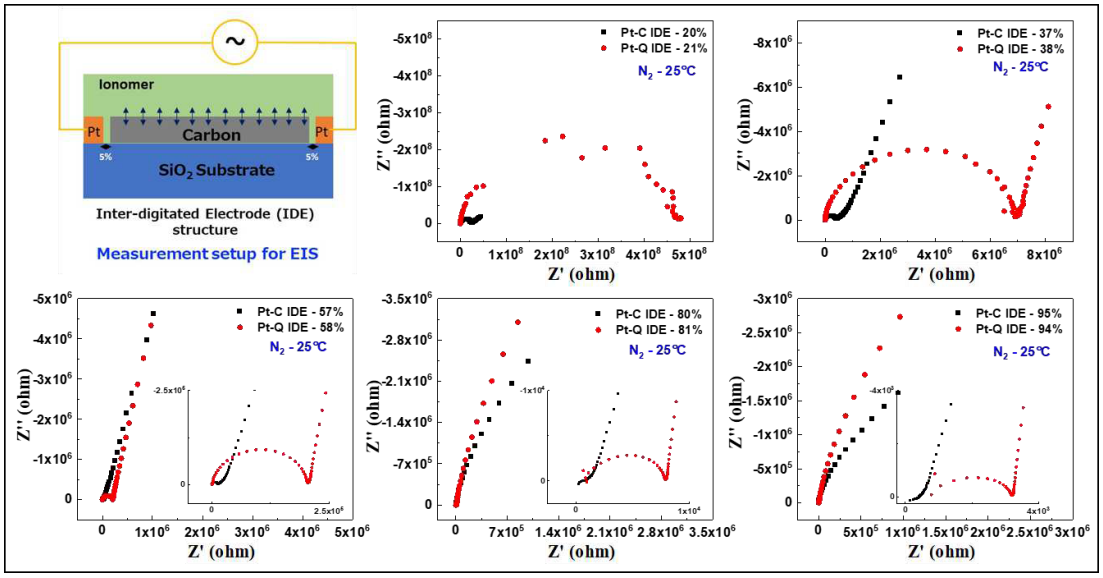

Figure 4. The Nyquist plots of Nafion thin film prepared on Pt-C IDE and Pt-Q IDE. The EIS measurement was performed at 25°C and various RH conditions in N_2 environment. The magnified plots are shown in figure insets at RH 58%, 80% and 95%.

The Nyquist plots show that the Nafion thin-film H^+ transport resistance in Pt-Q IDE is high compared to the Pt-C IDE at the same RH. In Pt-C IDE Nyquist plot, at high RH (80% & 90%) no semi-circle is observed in impedance plot which indicates high H^+ transport in Nafion film at carbon substrate since most area between the Pt electrodes is covered with carbon (91% area). In the Nyquist plots of Pt-C IDE, it is expected that there should be two responses corresponding to the ionomer/quartz (~9%) and ionomer/carbon (91%) interfaces. Approximately, 91% of the area between the Pt electrodes is carbon (100 µm) and the rest is quartz (10 µm) compared to Pt-Q IDE where the whole area between Pt electrodes is quartz (110 µm). So, the obtained H^+ transport impedance from Pt-C IDE could be attributed to quartz and carbon in a ratio of 1:9. Figure 5 shows the illustration for the attribution of obtained impedance in both IDEs. To obtain

the H^+ conductivity of Nafion thin-film on quartz and carbon pad in Pt-C IDE, it is important to normalize the obtained resistance values according to ionomer/substrate interfacial area.

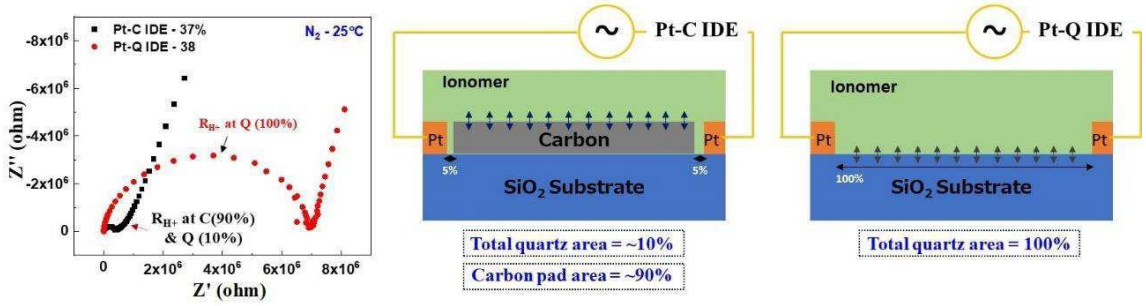

Figure 5. The Nyquist plot and illustrations of Pt-C IDE and Pt-Q IDE at 38% RH in N_2 environment and the attribution of H^+ transport impedance.

Firstly, the Nafion's H^+ conductivity at quartz from Pt-Q IDE and normalized H^+ conductivity at quartz from Pt-C IDE was estimated. In case of Pt-C IDE, to estimate the normalized H^+ conductivity at quartz and carbon, the *d* value (distance between electrode) was considered to be 10 µm (i.e., the distance representing the ionomer/quartz interfacial area) and 100 µm (i.e., the distance representing the ionomer/carbon interfacial area) respectively. Figure 6(a) illustrates the IDEs structure and equation for H^+ conductivity estimation with normalized *d* value for both IDEs. Figure 6(b) shows averaged H^+ transport resistance obtained by ZView fitting from Pt-Q IDEs and Pt-C IDEs with error bars. The proton transport resistance from IDE with carbon pad is approximately one order of magnitude lower than the IDE with quartz interface. It suggests that the Nafion H^+ transport property is affected by the substrates and supports the previous research on the substrate dependent changes in thin-film H^+ transport (21–23,25). To understand the attribution of enhanced H^+ transportation in Pt-C IDE, the H^+ conductivity at quartz and carbon from impedance data was estimated using normalized d value and compared with the H^+ conductivity on quartz from Pt-Q IDE. The H^+ conductivity at quartz in Pt-C IDE and Pt-Q IDE is shown in Fig 6(c). Interestingly, the Nafion's H^+ conductivity values at quartz are comparable in each IDEs at RH < 90% however at 90% and 95% RH, the H^+ conductivity in Pt-C IDE does not increases expectedly and shows saturation.

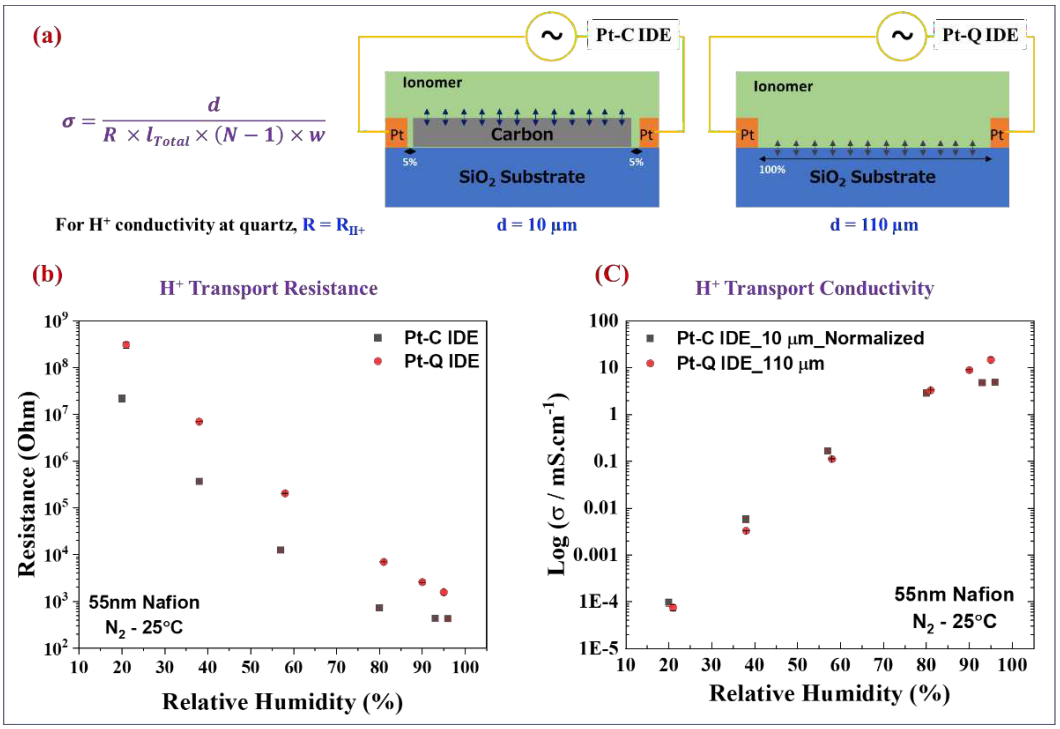

Figure 6. (a) Shows the equation and illustration for the normalization of H^+ conductivity at quartz in Pt-Q IDE and Pt-C IDE. (b) The averaged H^+ transport resistance of Nafion thin film in IDEs with error bars (EIS measurement was recorded with two separate IDEs). (c) The normalized H^+ conductivity (averaged) at quartz in Pt-C IDE compared with H^+ conductivity at quartz from Pt-Q IDE with error bar (EIS measurement was recorded with two separate IDEs).

The H^+ conductivity value at quartz from Pt-Q IDE (at 95% RH) and Pt-C IDE (at 94% RH) is 15 mS cm^{-1} and 4.9 mS cm^{-1} respectively. The reason for lower H^+ conductivity at quartz in Pt-C IDE at high RH (>90%) is not clear. Further, the Nafion H^+ conductivity at carbon from Pt-C IDE was estimated from H^+ transport resistance using equation [1] with normalized d value (100 µm) according to the carbon/ionomer interfacial area. Figure 7 shows the H^+ conductivity at quartz in Pt-Q IDE and compared with the normalized H^+ conductivity at carbon in Pt-C IDE. The graph shows high H^+ conductivity at carbon substrate at the same RH. The proton conductivity of Nafion's thin film at carbon substrate was more than an order of magnitude higher than that of quartz substrate in low RH (20%). At 95% RH the conductivity at carbon stabilizes and reaches to 49 mS cm^{-1} compared to H^+ conductivity at quartz in Pt-Q IDE which shows conductivity value of 15 mS cm^{-1}. The H^+ conductivity value at quartz at high RH (95%) is matched with our lab's previous work (23). Devproshad K. Paul et. al., and our group

Yutaro Ono et. al., previously reported the H^+ conductivity of Nafion film of thickness 4-55 nm at quartz with Au-Q IDE and Nafion film of 75 nm thickness on parallel electrodes respectively, showed similar H^+ conductivity at high RH (95%) (23,24). However, at low RH (20% and 40%) the H^+ conductivity value at quartz substrate shows slightly lower values in presented result (Fig. 7) than the previous research (24). Since the thin-film preparation method and choice of electrode material is different, it is hard to explain the reason for slightly lower conductivity at low RH (20% and 40%). On the other hand, H^+ conductivity at carbon was also compared with previous work using Au-C IDEs of comparable geometry (22). Our results show approximately one-order magnitude higher H^+ conductivity on carbon substrate. The H^+ conductivity strongly correlated with the water uptake content however the water uptake content of Nafion thin film over carbon and quartz substrate do not show very high-water uptake content (21). Thus, it can be concluded that the water uptake of Nafion film on SiO_2 and carbon are not remarkably different to explain the increase in conductivity.

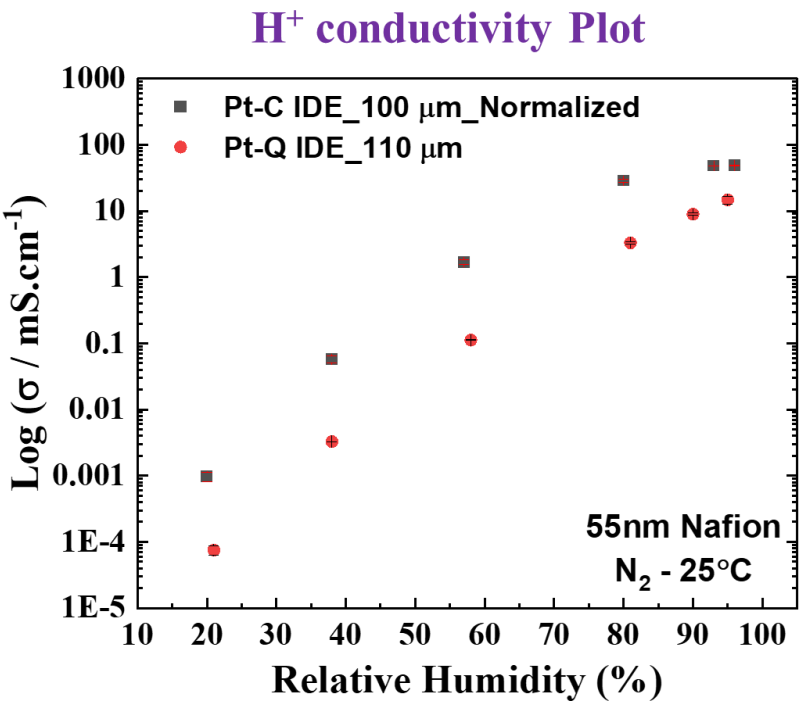

Figure 7. (a) The normalized H^+ conductivity at carbon in Pt-C IDE and at quartz in Pt-Q IDE with error bar. Normalization distance between Pt electrodes is mentioned in figure text.

Similarly, Gao et. al., estimated H^+ conductivity of Nafion thin-film (50 nm) over

carbon substrate using Au-C IDE of comparable geometry in N_2 environment and shows an order magnitude lower of H^+ conductivity at 95% RH (22). Interestingly at low RH (20%), there is approximately two order magnitude difference in H^+ conductivity in our results than the reported values from Gao et. al. work. Although this comparison of H^+ conductivity at carbon is not completely reasonable as electrode material, Nafion dispersion solvent, IDEs geometry, quality of carbon pad is different (resistance and structure) and thin-film pretreatment condition is unclear.

Comparing our results with previous work on H^+ conductivity at carbon substrate from one of coauthors' work, the significant increase in H^+ conductivity in Pt-C IDE cannot be explained (21). Moreover, the normalized H^+ conductivity at quartz from Pt-C IDE and H^+ conductivity at quartz in Pt-Q IDE shows similar values. It indicates that the obtained H^+ transport resistance from Pt-C IDE is truly H^+ transport resistance at quartz only, and the normalized resistance is comparable with the resistance from Pt-Q IDE which is also supported by the work recently published by Karan's group (21). They concluded that in N_2 environment, the H^+ transport resistance over carbon substrate is absent and can only be obtained in H_2 environment using Pt IDE. Therefore, H^+ conductivity measurement of Nafion's thin-film using either Pt-Q IDE or Pt-C IDE results in H^+ conductivity over quartz substrate. In our results, the reason for lower H^+ conductivity at high RH is unknown and will be further investigated with various carbon pad widths to understand the effect of carbon pad on Nafion H^+ conductivity in detail.

Conclusions

Substrate dependent H^+ conductivity of Nafion thin film has the potential to understand the attribution of elements of the catalyst layer for fuel cell performance enhancement. Previous studies have shown the H^+ conductivity of Nafion on Pt, C and quartz using Au and Pt based IDEs however the attribution of elements is still poorly understood. In this work, in-plane proton transport of Nafion thin film was investigated and the attribution of H^+ transportation on carbon and quartz using Pt-C IDE and Pt-Q IDE in N_2 environment was proposed. The Pt IDEs were fabricated with high precision and reproducible geometry. The current-voltage response of IDEs in range of 0-1 V was found to be in femtoampere (fA). For the first time, the morphology of spin-coated Nafion thin- film was shown and it is accustomed to the similar IDE morphology. H^+ transport of spin coated Nafion thin film (~55 nm) was measured by EIS in N_2 environment. The attribution of H^+ transport resistance was quantitatively decided to calculate the H^+ conductivity in Pt-C IDE. The normalized H^+ conductivity was obtained from resistance of Pt-C IDE Nyquist plots based on carbon/ionomer and ionomer/quartz interfacial area between electrodes. The comparison of estimated H^+ conductivity at quartz from Pt-C

IDE after normalization (d value = 10 μm), and H^+ conductivity from Pt-Q IDE shows comparable values except at the high RH. The H^+ conductivity at carbon substrate cannot be estimated as the H^+ transport resistance at carbon is absent in N_2 environment, and this work was supported by the previous research from Kunal's group. The result supports the quantitative attribution of resistance to estimate the H^+ conductivity at quartz substrate. Nafion's H^+ conductivity at carbon can be estimated from the measurements under H_2 environment and will be estimated in future work.

Acknowledgments

This work was supported by research funding from JSPS KAKENHI Grant Number JP21H00020, The Murata Science Foundation, and JST CREST Grant Number JPMJCR21B3.

References

1. S. A. Grigoriev, V. I. Porembsky, and V. N. Fateev, *Int. J. Hydrogen Energy* **31**(2), 171–175 (2006).
2. S. Holdcroft, *Chem. Mater.* **26**(1), 381–393 (2014).
3. Y. Wang, K. S. Chen, J. Mishler, S. C. Cho, and X. C. Adroher, *Appl. Energy* **88**(4), 981–1007 (2011).
4. W. Y. Hsu and T. D. Gierke, *J. Memb. Sci.* **13**(3), 307–326 (1983).
5. K. A. Mauritz and R. B. Moore, *Chem. Rev.* **104**(10), 4535–4585 (2004).
6. A. Kusoglu and A. Z. Weber, *Chem. Rev.* **117**(3), 987–1104 (2017).
7. M. Lopez-Haro, L. Guetaz, T. Printemps, A. Morin, S. Escribano, P. H. Jouneau, P. Bayle-Guillemaud, F. Chandezon, and G. Gebel, *Nat. Commun.* **5** 5529 (2014).
8. Y. Nagao, *Sci. Technol. Adv. Mater.* **21**(1), 79–91 (2020).
9. K. Karan, *Langmuir* **35**(42), 13489–13520 (2019).
10. D. K. Paul, K. Karan, A. Docoslis, J. B. Giorgi, and J. Pearce, *Macromolecules* **46**(9), 3461–3475 (2013).
11. K. Karan, *ECS Trans.* **50**(2), 395–403 (2013).

12. K. Karan, *Curr. Opin. Electrochem.* **5**(1), 27–35 (2017).
13. A. Kusoglu, T. J. Dursch, and A. Z. Weber, *Adv. Funct. Mater.* **26**(27), 4961–4975 (2016).
14. H. F. M. Mohamed, S. Kuroda, Y. Kobayashi, N. Oshima, R. Suzuki, and A. Ohira, *Phys. Chem. Chem. Phys.* **15**(5), 1518–1525 (2013).
15. M. A. Modestino, D. K. Paul, S. Dishari, S. A. Petrina, F. I. Allen, M. A. Hickner, K. Karan, R. A. Segalman, and A. Z. Weber, *Macromolecules* **46**(3), 867–873 (2013).
16. Y. Nagao, *J. Phys. Chem. C* **117**(7), 3294–3297 (2013).
17. Y. Nagao, *e-Journal Surf. Sci. Nanotechnol.* **10**, 114–116 (2012).
18. V. S. Murthi, J. Dura, S. Satija, and C. Majkrzak, *ECS Trans.* **16**(2), 1471–1485 (2008).
19. U. N. Shrivastava, K. Suetsugu, S. Nagano, H. Fritzsche, Y. Nagao, and K. Karan, *Soft Matter* **16**(5), 1190–1200 (2020).
20. H. Kang, S. H. Kwon, R. Lawler, J. H. Lee, G. Doo, H.-T. Kim, S.-D. Yim, S. S. Jang, and S. G. Lee, *J. Phys. Chem. C* **124**(39), 21386–21395 (2020).
21. U. N. Shrivastava, D. Khattar, C. Kendrick, and K. Karan, *J. Electrochem. Soc.* **167**(13), 134520 (2020).
22. X. Gao, K. Yamamoto, T. Hirai, N. Ohta, T. Uchiyama, T. Watanabe, M. Takahashi, N. Takao, H. Imai, S. Sugawara, K. Shinohara, and Y. Uchimoto, *Solid State Ionics* **357**, 115456 (2020).
23. Y. Ono and Y. Nagao, *Langmuir* **32**(1), 352–358 (2016).
24. D. K. Paul, R. McCreery, and K. Karan, *J. Electrochem. Soc.* **161**(14), F1395–F1402 (2014).
25. S. C. DeCaluwe, A. M. Baker, P. Bhargava, J. E. Fischer, and J. A. Dura, *Nano Energy* **46**, 91–100 (2018).